Molecular adsorption study of nicotine on the nitrogen doped TiO_2 anatase nanoparticles: Insights from van der Waals corrected DFT computations

Amirali Abbasi* & Jaber Jahanbin Sardroodi

Molecular Simulation laboratory (MSL), Computational Nanomaterials Research Group (CNRG),
Department of Chemistry, Azarbaijan Shahid Madani University, Tabriz, Iran
Email: a_abbasi@azaruniv.edu

The interaction of nicotine with undoped and nitrogen-doped TiO_2 anatase nanoparticles is investigated by density functional theory studies. The results indicate that the interaction between nicotine and N-doped TiO_2 nanoparticles is stronger than that between nicotine and pristine TiO_2 nanoparticles, which suggests nitrogen doping helps to strengthen the interaction of nicotine with TiO_2 nanoparticles. In other words, the doping of nitrogen atom promotes the interaction of nicotine with TiO_2 nanoparticles. It is found that the nitrogen atom of nicotine molecule tends to be strongly adsorbed on the five-fold coordinated titanium site of N-doped anatase nanoparticles. By including van der Waals interactions between nicotine molecule and TiO_2, it is found that the adsorption on the N-doped TiO_2 is energetically more favorable than that on the pristine one. The projected density of states analysis indicates the formation of chemical bond between nitrogen atom of nicotine and titanium atom of nanoparticle. These results offer a theoretical basis and general understanding of the interaction of TiO_2 nanoparticles with nicotine, suggesting potential applications of N-doped TiO_2 nanoparticles in designing of novel sensors and removers for nicotine detection.

Titanium dioxide (Titania) is one the most important semiconductor materials, having diverse applications in numerous aspects including photo-catalysis[1], gas sensor devices, heterogeneous catalysis[2] and photovoltaic cells[3]. This substantially well-ordered metal oxide is the most widely used material during the past decades due to its excellent properties such as nontoxicity, chemical stability, extensive band-gap and so on[4-8]. Numerous researchers have focused on studying important properties of TiO_2[8-15]. The wide band gap of TiO_2 anatase (3.2 eV) restricts its photocatalytic activity and it can only absorb a lower percentage (3–5%) of the received solar light. An efficient strategy towards improving the photocatalytic properties of TiO_2 would be a procedure that increases the optical sensitivity of TiO_2 to the visible area. Doping of TiO_2 with some non-metal elements such as nitrogen is one process, which greatly increases the photocatalytic activity of TiO_2[16-19].

Several computational and experimental studies have been reported on the N-doped TiO_2 anatase nanoparticles over the past few years. For example, Liu *et al.*[20] reported the adsorption of NO molecules on the N-doped nanoparticles. Doping of TiO_2 nanoparticles with nitrogen atom rectified its electronic and structural properties and made it possible for the TiO_2 to be used in gas sensor devices[20-25]. The effects of N-doping on electronic structure of TiO_2 anatase and the photocatalytic activity have been investigated in some other works[26,27].

Health hazards due to cigarette smoking is widely known. There are many harmful and carcinogenic compounds in cigarette smoke, especially nicotine, which causes hazardous effects on public and human health. Thus, efficiency of systems for sensing nicotine molecule is necessary because of its side effects on both the smoker as well as the other people in the vicinity[29]. Nicotine is an alkaloid and therapeutic compound, which can have potent and stimulant effects on the central nervous system and is commonly utilized by human beings as an addictive drug. Nicotine has positive impacts on the nervous cell performance in the early stages of consumption. However, in the long run, it could cause irreparable effects on the body. So, the design of an efficient sensor for nicotine removal is an important issue to

human safety[28, 29]. To fully examine the effects of the nicotine adsorption on the structural and electronic properties of TiO$_2$, as well as the effects of nitrogen doping, theoretical investigations have also been conducted[14,19,30].

In this research, the interaction of nicotine with N-doped TiO$_2$ anatase nanoparticles was investigated using the DFT computations. The electronic and structural properties of the complex systems and the adsorption energies in adsorbed complexes were computed and analyzed. Furthermore, the effects of doping of nitrogen on total and projected density of states of TiO$_2$ were investigated in detail.

Methodology

Computation

The DFT calculations presented in this work[31,32] were carried out using the Open source Package for Material eXplorer (OPENMX) ver. 3.8, which was found to be an effective and well organized software package for nano-scale material simulations based on density functional theories, and pseudo-atomic localized basis functions[33]. Pseudo-atomic orbitals (PAO's) centered on atomic sites were employed as basis sets in order to expand the wave functions in a KS schema with a cutoff energy of 150 Ry (Rydberg)[33,34]. These PAOs were generated by using the basis sets (two *s*, two *p*, one *d*) for Ti atom, two *s* and two *p* for O, N and C atoms and two *s* for H atom according to the cutoff radii set to the values of 7 for Ti, 5 for O, N and C and 5.5 for H, (all in Bohrs) generated by a confinement scheme. The generalized gradient approximation functional (GGA) in the Pedrew-Burke-Ernzerhof (PBE) form was used in order to describe the exchange-correlation energy functional[35]. The van der Waals interactions were examined using the DFT-D2 method. An effective open-source program (XCrysDen)[36] was utilized for visualizing the isosurfaces such as molecular orbitals, contours presented in this study. The adsorption energy was calculated by Eq. 1,

$$E_{ad} = E_{(particle+Nicotine)} - E_{particle} - E_{Nicotine)} \qquad \dots (1)$$

where $E_{(particle+Nicotine)}$, $E_{particle}$ and $E_{Nicotine}$ are the energies of the complex system, the free TiO$_2$ nanoparticle without any adsorbed molecule and the free nicotine molecule in a non-adsorbed state respectively. The more negative the E_{ad} is, the more energy favorable the adsorbed structure is.
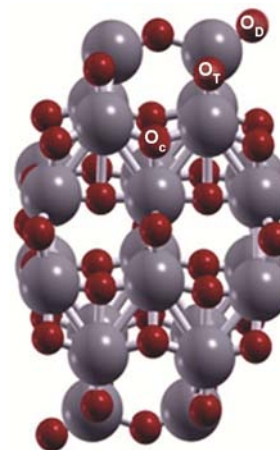

Fig. 1–Optimized structure of a pristine TiO$_2$ anatase nanoparticle constructed from the 3×2×1 unit cells. [O$_C$: central oxygen; O$_T$: twofold coordinated oxygen; O$_D$: dangling oxygen].

Models of nanoparticles

The considered TiO$_2$ anatase nanoparticles containing 72 atoms (24 Ti and 48 O atoms) were constructed by placing 3×2×1 numbers of TiO$_2$ unit cells along *x*, *y* and *z* axis, respectively (Fig. 1). The unit cell was derived from the "American Mineralogists Database" webpage[37] and reported by Wyckoff[38]. N-doped TiO$_2$ anatase nanoparticles were built by substituting two surface oxygen atoms by nitrogen atoms. The crystal model of TiO$_2$ anatase nanoparticle contains two types of titanium atoms, referred to as five-fold coordinated Ti (5*f*-Ti) and six-fold coordinated Ti (6*f*-Ti) atoms, as well as two types of oxygen atoms, specified by three-fold coordinated O (3*f*-O) and two-fold O (2f-O) atoms. Generally, the 2*f*-O and 5*f*-Ti atoms are more reactive than the 3*f*-O and 6*f*-Ti atoms because of their unsaturated coordination. The substitution of oxygen atom by nitrogen atom in the TiO$_2$ nanoparticle leads to introduction of a hole in the particle as displayed in the front and side views of Fig. 2. We have investigated the adsorption of oxygen on the active five-fold coordinated titanium sites of the TiO$_2$ anatase nanoparticles due to their relatively high activity in the adsorption process in comparison with the other oxygens. The nicotine molecule preferentially interacts with the cationic titanium sites and the adsorption on the five-fold coordinated titanium sites provides the most stable adsorption configurations. The structure of the nicotine molecule before the adsorption is shown in Fig. 3.
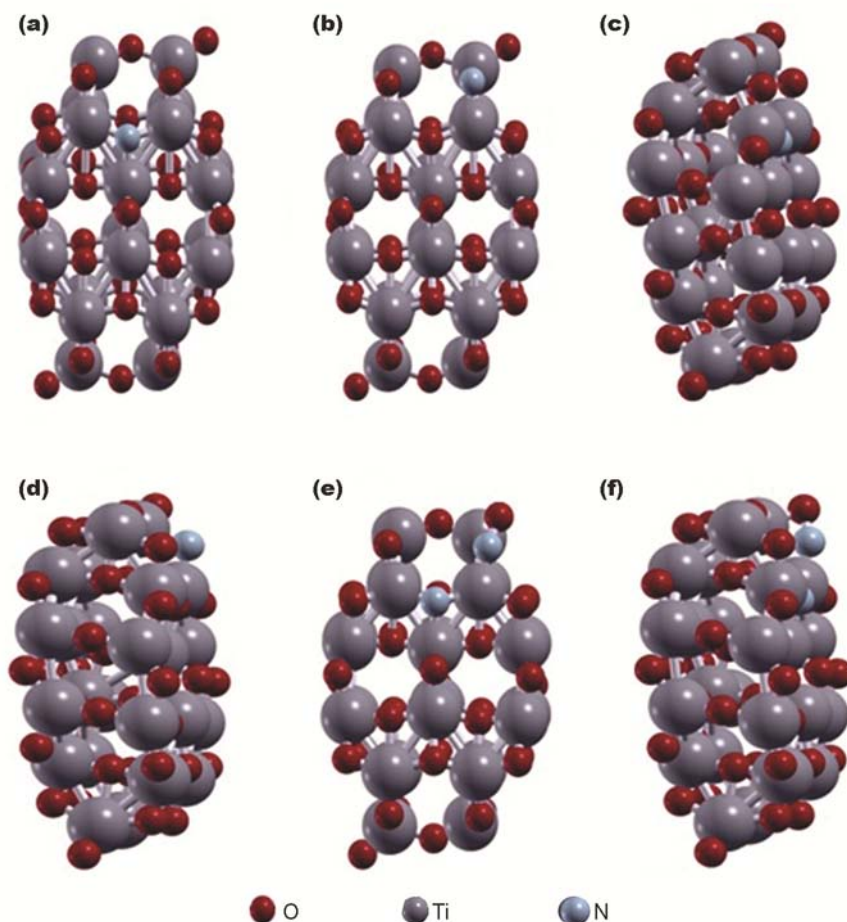
Fig. 2–Optimized N-doped TiO_2 anatase nanoparticles constructed from the $3\times2\times1$ unit cells in front and lateral views. [(a) O_C-substituted nanoparticle in front view; (b) O_T-substituted nanoparticle in front view; (c) O_C-substituted nanoparticle in side view; (d) O_T-substituted nanoparticle in side view; (e) $O_{C,\ T}$-substituted nanoparticle in front view; (f) $O_{C,\ T}$-substituted nanoparticle in side view].
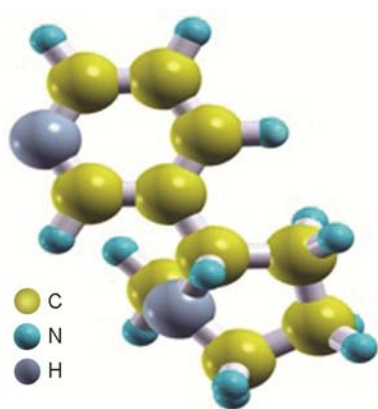

Fig. 3–Representation of the nicotine molecule before the adsorption process.

Results and Discussion

Structural analysis

The adsorption of nicotine molecule on the five-fold coordinated titanium site of TiO_2 was considered. In the presented configurations, the nitrogen atom of nicotine was placed perpendicularly towards the nanoparticle, resulting in the adsorption on the nanoparticle with slight distortion but with the same orientation (perpendicular). Both these interactions include N-doped nanoparticles in the middle oxygen position and N-doped ones in the two-fold coordinated oxygen atom sites.

The coverage effect of nitrogen doping was also examined here, which suggests that two nitrogen
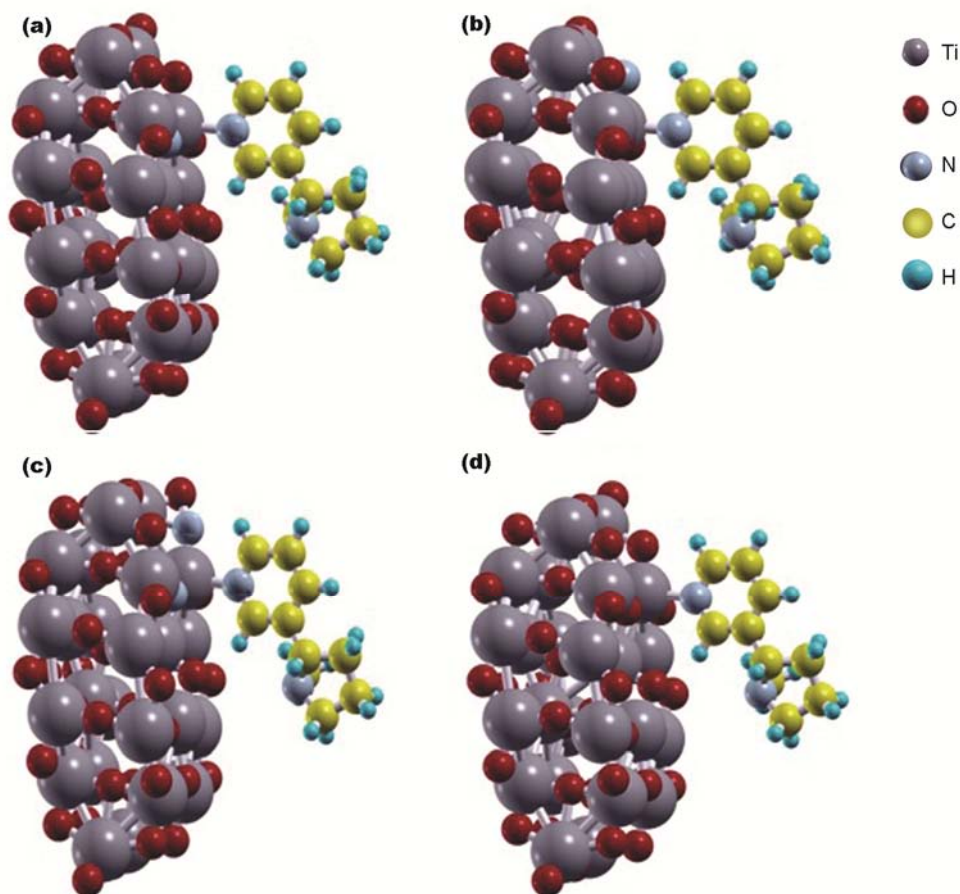
Fig. 4–Optimized TiO$_2$-nicotine configurations with perpendicular orientations of Nicotine molecule towards the TiO$_2$ nanoparticle.

atoms makes TiO$_2$ nanoparticle more active than one nitrogen atom[20]. In other words, substitution of two oxygen atoms of TiO$_2$ by two nitrogen atoms increases its reactivity and adsorption ability for the nicotine molecule. The coverage effect refers to substitution of the oxygen atoms of TiO$_2$ by nitrogen atoms (N doping) and indicates the number of doped nitrogen atoms in the particle. The adsorption of nicotine molecule was also considered on the O$_{C,T}$-substituted (two-N-doped) TiO$_2$ nanoparticle in order to analyze the effect of further nitrogen doping on the adsorption energetic (as well as geometries) of nicotine molecule at TiO$_2$ nanoparticle surface.

Figure 4 illustrates the optimized TiO$_2$-nicotine configurations in perpendicular position. Four configurations, namely A to D, were considered for the nicotine-adsorbed systems in perpendicular configuration. For example, configuration B was made from the O$_T$-substituted TiO$_2$ nanoparticle and nicotine molecule in vertical orientation

Table 1 – Bond lengths, adsorption energies and Mulliken charge results for the interaction of nicotine with N-doped TiO$_2$ anatase nanoparticles

Complex	Newly-formed Ti-N (Å)	ΔE_{ad} (eV)		ΔQ (|e|)
		PBE	DFT-D2	
(A)	2.35	−10.90	−13.90	-0.783
(B)	2.30	−10.95	−14.20	-0.609
(C)	2.22	−11.82	−14.82	-0.417
(D)	2.29	−8.37	−11.20	-0.380

towards the nanoparticle. The optimization of the configurations formed from the nicotine molecule adsorbed on the five-fold coordinated titanium atom site leads to configurations which have more negative adsorption energy and higher stability. Thus, the most stable configuration (perpendicular) was investigated in this study. It was found that the perpendicular interaction of nicotine with TiO$_2$ nanoparticles leads to the most stable configuration with greater degree of favorability. The optimized values of the newly-formed Ti-N bond between titanium atom of nanoparticle and nitrogen atom of

nicotine molecule are listed in Table 1. As can be seen from this table, the configuration C has the smallest Ti-N bond length value, as compared to the other configurations. This is in line with the higher adsorption energy of this configuration in comparison with the other configurations. The smaller the bond formed between the nitrogen atom of nicotine molecule and the five-fold coordinated titanium atom of nanoparticle (Ti-N), the stronger is the interaction of nicotine with TiO_2 nanoparticle. Since a higher adsorption energy results in a stronger binding between adsorbate and the nanoparticle, there is a stronger interaction between nicotine and TiO_2 nanoparticle in configuration C as compared to the other complexes. Also, a lower newly formed Ti-N bond in configuration B corresponds to the higher value of adsorption energy, which suggests that the nicotine molecule strongly interacts with TiO_2 nanoparticle in configuration B as compared to configuration A. Adsorption energy analysis shows that the interaction of nicotine molecule with N-doped nanoparticle is stronger than the interaction with undoped nanoparticle. This means that the adsorption on the N-doped nanoparticles is the most energy favorable and provides the most stable configuration. As can be seen from Table 1, all the computed adsorption energies are significantly increased when the vdW interactions are considered in the calculations. Therefore, the adsorption energies of nicotine molecule on the undoped and nitrogen-doped TiO_2 nanoparticles becomes higher when the vdW interactions are included, suggesting significant domination of vdW interactions during the adsorption process.

The results also indicate that adsorption on N-doped nanoparticle with two nitrogen atoms is energetically more favorable than the adsorption on the N-doped nanoparticle with one nitrogen atom. A comparison of the results obtained for the adsorption on the pristine (undoped) nanoparticles with those obtained for the N-doped ones reveals that the interaction between N-doped nanoparticles and nicotine is stronger than that between undoped nanoparticle and nicotine molecule. It should be noted that the N-doped nanoparticle with two nitrogen atoms reacts with nicotine molecule more efficiently in comparison with the nanoparticle with one nitrogen atom. Therefore, the N doping strengthens the adsorption of nicotine on the TiO_2 nanoparticles. The results show that the adsorption energies of nicotine on the different nanoparticles follow the order: two-N-doped >N-doped >Pristine. Since the N-doped nanoparticles have higher sensing capabilities than the undoped ones, we can conclude that the N-doped nanoparticles are the most efficient candidates for applications in sensing of nicotine molecule.

Electronic properties

Figure 5 displays the total density of states (TDOS) for the interaction of nicotine with N-doped TiO_2 nanoparticles before and after the adsorption process. This figure shows that the main features are the formation of some small peaks at the energy ranges from –8 to –12 eV and changes in the energies of the states to the lower values after the adsorption. These changes in energy gap of DOS would affect the electronic transport properties of the nanoparticles and this feature can be beneficial for sensing of nicotine by TiO_2 nanoparticles.

The projected density of states (PDOSs) were computed to further analyze the nicotine adsorption on TiO_2 nanoparticles. The titanium and nitrogen projected DOSs (Ti-PDOS and N-PDOS) after the adsorption are displayed in Fig. 6(a-d) representing the PDOSs for the adsorption types A, B, C and D, respectively. The high overlap of the PDOSs of titanium and nitrogen atoms shows the formation of new Ti-N bond between the titanium atom of nanoparticle and nitrogen atom of nicotine. This indicates that the nicotine molecule is chemisorbed on the five-fold coordinated titanium site of TiO_2 nanoparticle. The PDOSs of nitrogen atom of nicotine molecule and its outer layer p orbitals in comparison with the PDOS of titanium atom are given in Fig. 7, which shows that the overlap between the PDOSs of titanium atom and $p1$ (P_X) orbital of nitrogen atom is higher than the overlap between the PDOSs of titanium and $p2$, $p3$ (P_Y, P_Z) orbitals of nitrogen. The PDOSs of nitrogen atom of nicotine before and after the adsorption process suggest the shifting of the energies of the states and consequently changing the energy gap of TiO_2 (Fig. 8).

For bare nicotine molecule, the HOMO and LUMO molecular orbitals are shown in Fig. 9. This figure represents the localization of HOMO molecular orbitals on the five member ring of nicotine molecule
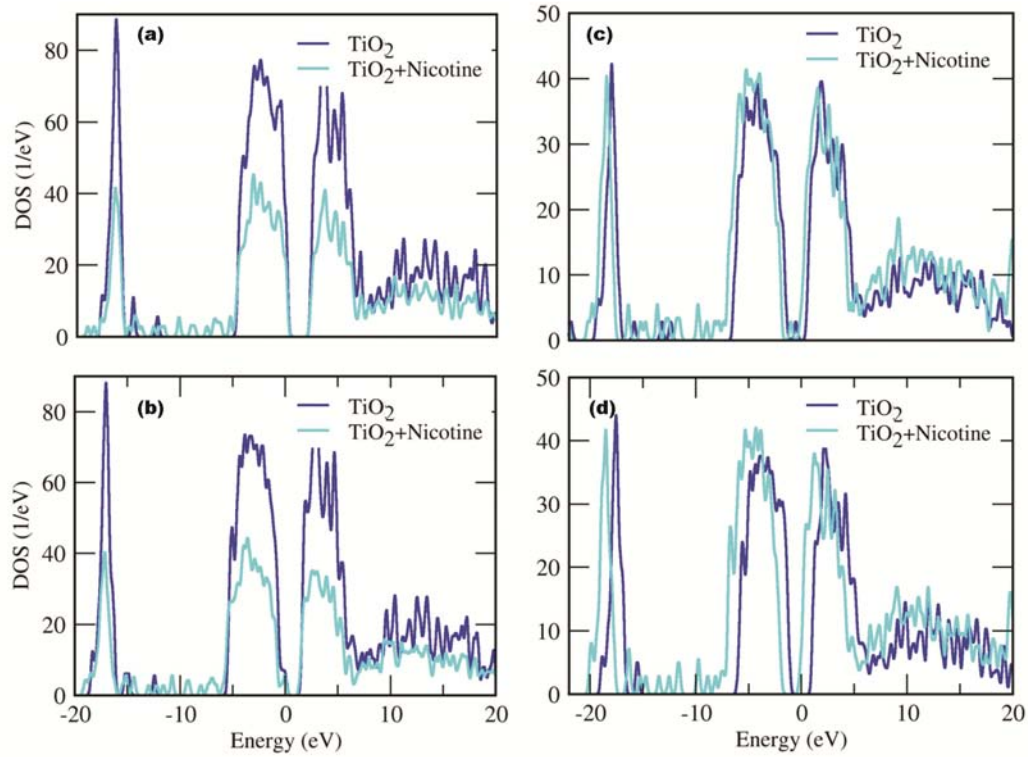
Fig. 5–DOS for the interaction of nicotine with N-doped TiO$_2$ anatase nanoparticle before and after the adsorption process. [(a) Complex A; (b) Complex B; (c) Complex C; (d) Complex D].
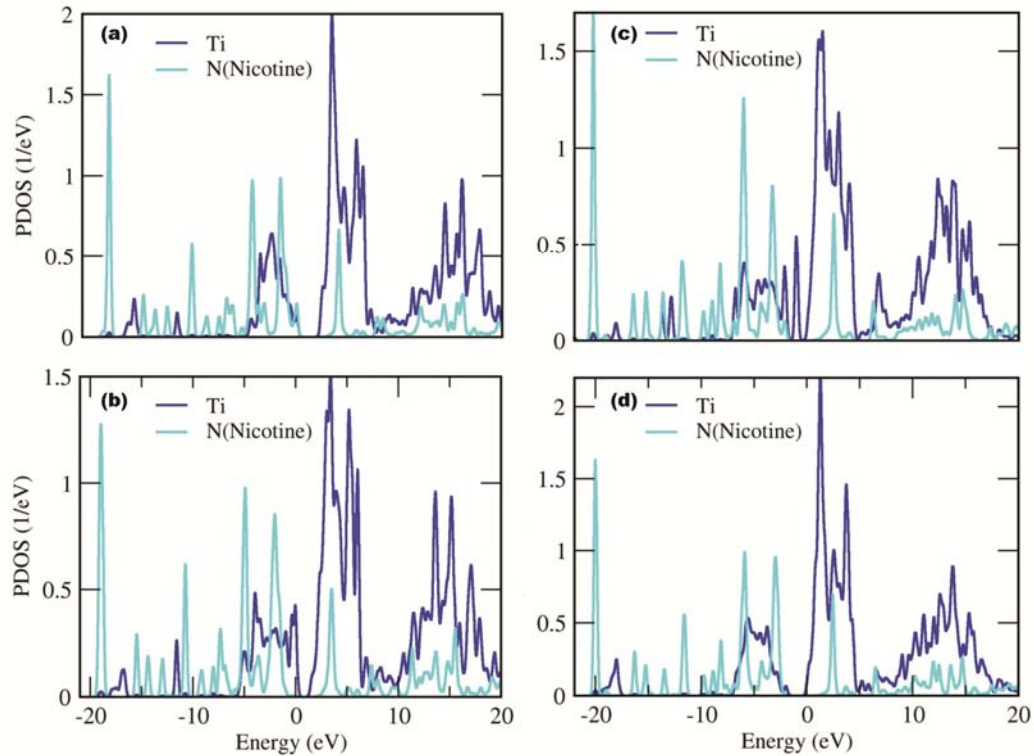

Fig. 6–PDOS for the interaction of nicotine with N-doped TiO$_2$ nanoparticles. [(a) Complex A; (b) Complex B; (c) Complex C; (d) Complex D].
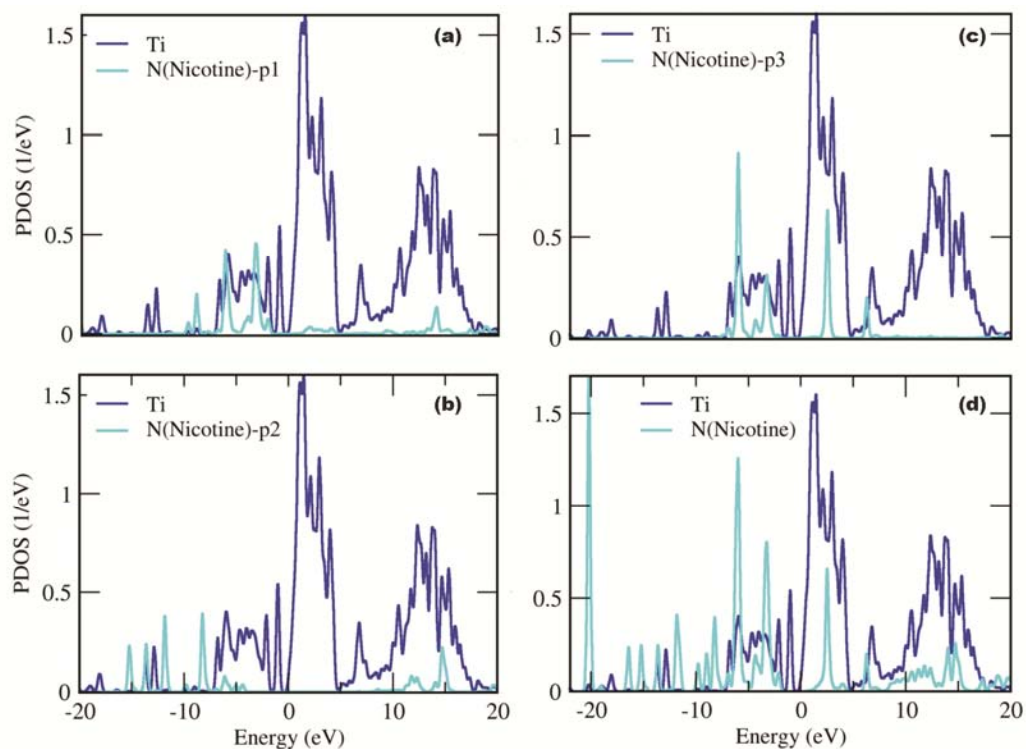
Fig. 7–PDOS of titanium, nitrogen and related *p* orbitals for adsorption type C. [(a) PDOSs of titanium and *p*1 orbital of nitrogen; (b) PDOSs of titanium and *p*2 orbital of nitrogen; (c) PDOSs of titanium and *p*3 orbital of nitrogen; (d) PDOSs of titanium and nitrogen].
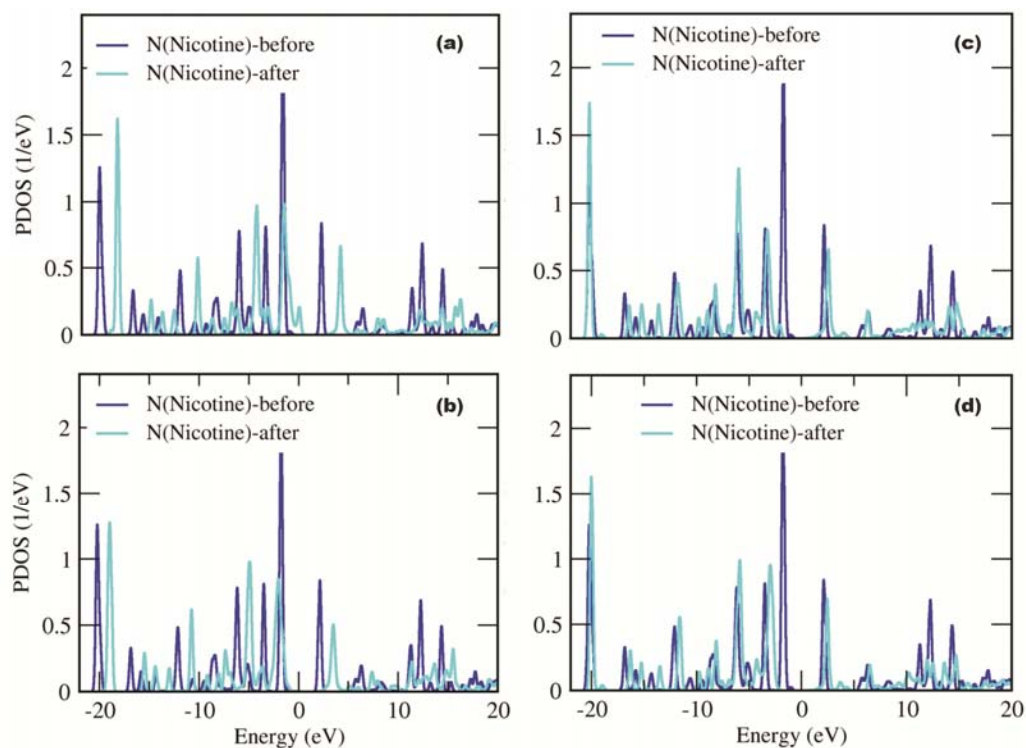

Fig. 8–PDOS of nitrogen atom of nicotine molecule before and after the adsorption process. [(a) Complex A; (b) Complex B; (c) Complex C; (d) Complex D].
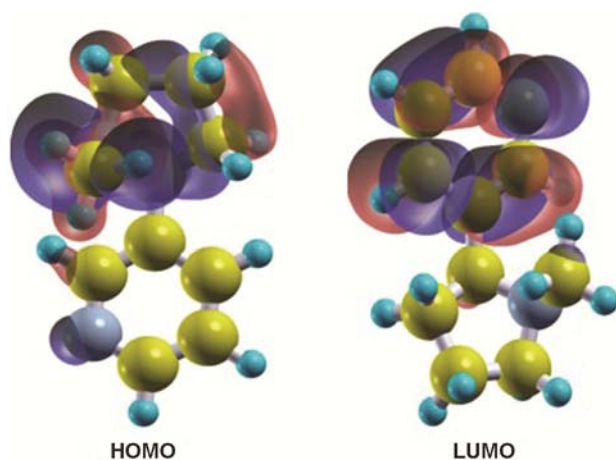
Fig. 9–The isosurfaces of HOMO and LUMO molecular orbitals for nicotine molecule before the adsorption process.

but the localization of the LUMO on the six member ring. The isosurfaces of molecular orbitals for TiO$_2$/Nicotine complexes are illustrated in Figs 10 and 11 respectively, which show that the HOMOs are mainly localized on the nicotine molecule, while the LUMOs are strongly localized on the TiO$_2$ nanoparticle.

To fully examine the charge transfer between nicotine and TiO$_2$ nanoparticle, the charge transfer analysis based on Mulliken charges was carried out (Table 1). In complex A, the calculated Mulliken charge value of TiO$_2$ nanoparticle is about -0.783 |e| (e, the electron charge) and that of nicotine molecule it is +0.783 |e|, which means that the TiO$_2$ nanoparticle acts as an electron acceptor and accepts electrons from nicotine. In the other complexes, we can see the same trend in charge transfer process. This charge transfer is expected to
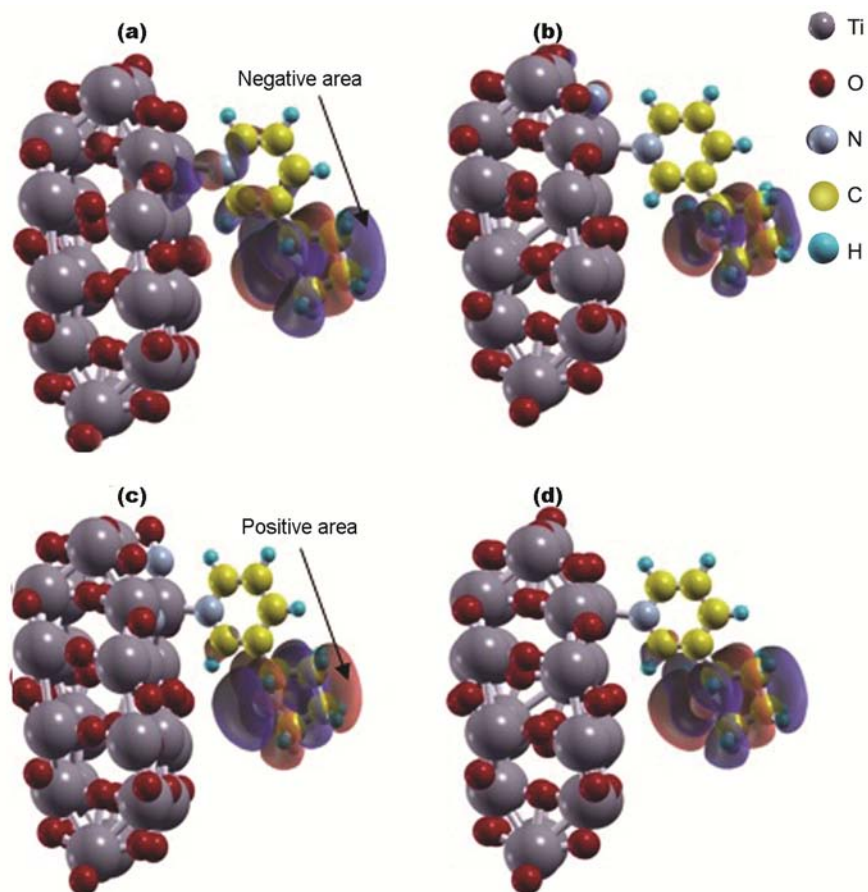

Fig. 10–The HOMO isosurfaces for TiO$_2$+nicotine configurations. [(a) Complex A; (b) Complex B; (c) Complex C; (d) Complex D].
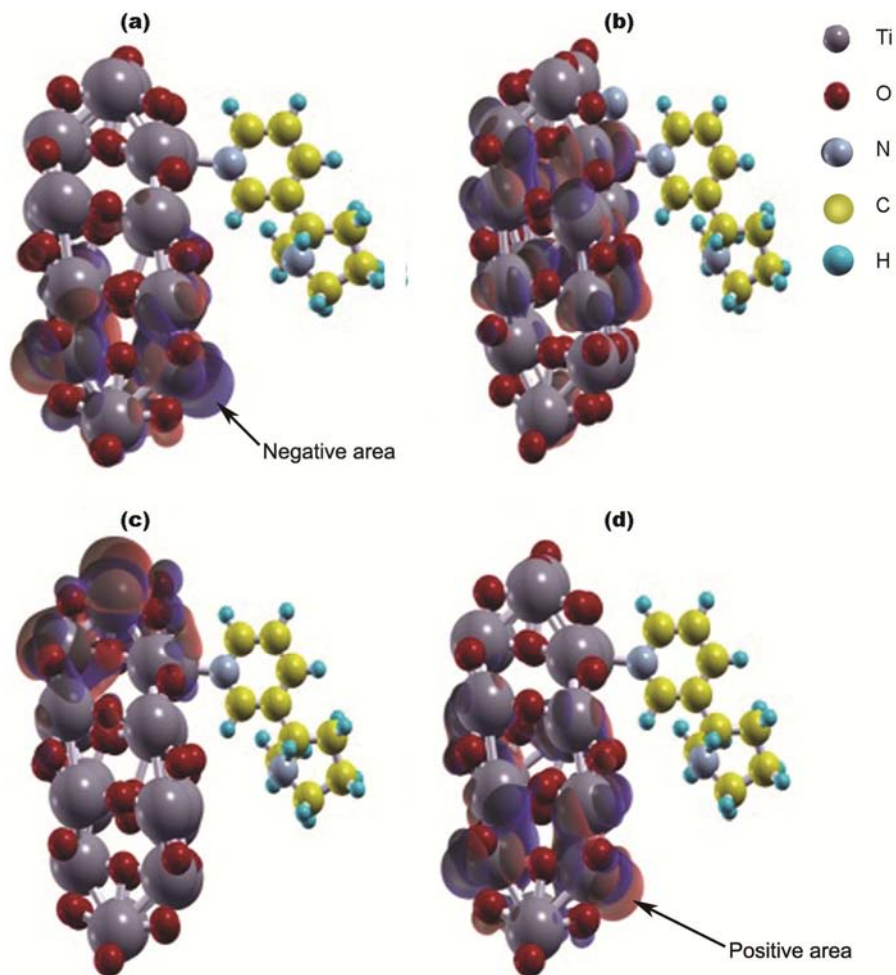
Fig. 11–The LUMO isosurfaces for TiO_2+nicotine configurations. [(a) Complex A; (b) Complex B; (c) Complex C; (d) Complex D].

cause changes on the conductivity of the system which would be helpful in the design and development of TiO_2-based biosensors for nicotine recognition.

Conclusions

The interactions of nicotine molecule with undoped and N-doped TiO_2 anatase nanoparticles were investigated by DFT computations. Analysis of the adsorption energies reveals that the interaction of nicotine with N-doped TiO_2 nanoparticle is stronger than that with undoped nanoparticle, i.e., the N-doped nanoparticles can interact with nicotine molecules more efficiently in comparison with the undoped ones. On including the vdW interactions in the calculations, it was concluded that the nicotine molecule is preferentially chemisorbed on the five-fold coordinated titanium site of TiO_2 nanoparticle. Moreover, the adsorption on the N-doped nanoparticles is energetically more favorable than the adsorption on the pristine nanoparticles. Also, the changes in the electronic structure due to the nicotine adsorption is assumed to be responsible for the strong interaction of nicotine molecule with TiO_2 nanoparticles, which suggests that N-doped TiO_2 can be efficiently used for adsorbing and sensing of nicotine. The PDOS and molecular orbital calculations demonstrate the formation of new chemical bonds at the interface between the nanoparticle and nicotine molecule.

Acknowledgement

References

1 Linsebigler A L, Lu G & Yates J T, *Chem Rev*, 95 (1995) 735.
2 Diebold U, *Surf Sci Rep*, 48 (2003) 53.

3   Fujishima A, Zhang X & Tryk D A, *J Surf Sci Rep*, 63 (2008) 515.

4   Henderson M A, *J Surf Sci Rep*, 66 (2011) 185.

5   Banfied J F & Veblen D R, *J Am Mineral*, 77 (1992) 545.

6   Grätzel M, *Nature*, 414 (2001) 338.

7   Fujishima A & Honda K, *Nature*, 37 (1972) 238.

8   Dutta P K, Ginwalla A, Hogg B, Patton B R, Chwieroth B, Liang Z, Gouma P, Mills M & Akbar S, *J Phys Chem*, 103 (1999) 4412.

9   Liu R, Zhou X, Yang F & Yu Y, *J Appl Surf Sci*, 319 (2014) 50.

10 Liu H, Zhao M, Lei Y, Pan C & Xiao W, *J Comput Mater Sci*, 15 (2012) 389.

11 Erdogan R, Ozbek O & Onal I, *J Surf Sci*, 604 (2010) 1029.

12 Onal I, Soyer S & Senken S, *J Surf Sci*, 600 (2006) 2457.

13 Wei Z, Mei W, Xiyu S, Yachao W & Zhenyong L, *J Semicond*, 31 (2010) 072001.

14 Liu J, Dong L, Guo W, Liang T & Lai W, *J Phys Chem C*, 117 (2013) 13037.

15 Zhao D, Huang X, Tian B, Zhou S, Li Y & Du Z, *J Appl Phys Lett*, 98 (2011) 162107.

16 Tang S & Cao Z, *J Chem Phys*, 134 (2011) 044710.

17 Rumaiz A K, Woicik J, Cockayne C E, Lin H Y, Jaffari G H & Shah S I, *J Appl Phys Letts*, 95 (2009) 262111.

18 Chen Q, Tang C & Zheng G, *J Phys B: Cond Mat*, 404 (2009) 1074.

19 Jia L, Wu C, Han S, Yao N, Li Y, Li Z, Chi B, Pu J & Jian L, *J Alloys Comp*, 509 (2011) 6067.

20 Liu J, Liu Q, Fang P, Pan C & Xiao W, *J Appl Surf Sci*, 258 (2012) 8312.

21 Li Y F, Aschauer U, Chen J & Selloni A, *J Acc Chem Res*, 47 (2014) 3361.

22 Berger T, Sterrer M, Diwald O, Knözinger E, Panayotov D, Thompson T L & Yates-Jr J T, *J Phys Chem B*, 109 (2005) 6061.

23 Mirzaei M, Ahadi H, Shariaty-Niassar M & Akbari M, *Int J Nanosci Nanotechnol,* 11 (2015) 289.

24 Zarei H, Zeinali M, Ghourchian H & Eskandari K, *Int J Nano Dimens*, (2013) 69.

25 Asantharaja D V, Ramalingam V & Reddy G A, *Nanomed J*, (2015) 46.

26 Hummatov R, Gulseren O, Ozensoy E, Toffoli D & Ustunel H, *J Phys Chem,* 116 (2012) 6191.

27 Livraghi S, Paganini M C, Giamello E, Selloni A, Valentin C D & Pacchioni G, *J Am Chem Soc*, 128 (2006) 15666.

28 Hyung-June L, Gunn K & Young-kyun K, *Chem Phys Lett*, 580 (2013) 57.

29 Girão E C, Fagan S B, Zanella I & Souza Filho A G, *J Hazard Mater*, 184(1-3) (2010) 678.

30 Shi W, Chen Q, Xu Y, Wu D & Huo C F, *J Solid State Chem*, 184 (2011) 1983.

31 Hohenberg P & Kohn W, *J Phys Rev*, 136 (1964) B864.

32 Kohn W & Sham L, *J Phys Rev*, 140 (1965) A1133.

33 *OPENMX, Pseudoatomic Basis Functions, and Pseudopotentials*, available at 'http://www.openmxsquare.org.

34 Ozaki T, *J Phys Rev B*, 67 (2003) 155108.

35 Perdew J P, Burke K & Ernzerhof M, *J Phys Rev Letts*, 78 (1997) 1396.

36 Koklj A, *J Comput Mater Sci*, 28 (2003) 155.

37 *American Mineralogists Database*, http://rruff.geo.arizona.edu/AMS/amcsd.php.

38 Wyckoff R W G, *Crystal Structures*, (Interscience Publishers, USA) 1963.